

Performance analysis of Lithium-ion-batteries: status and prospects

DPG conference Erlangen
March 2018

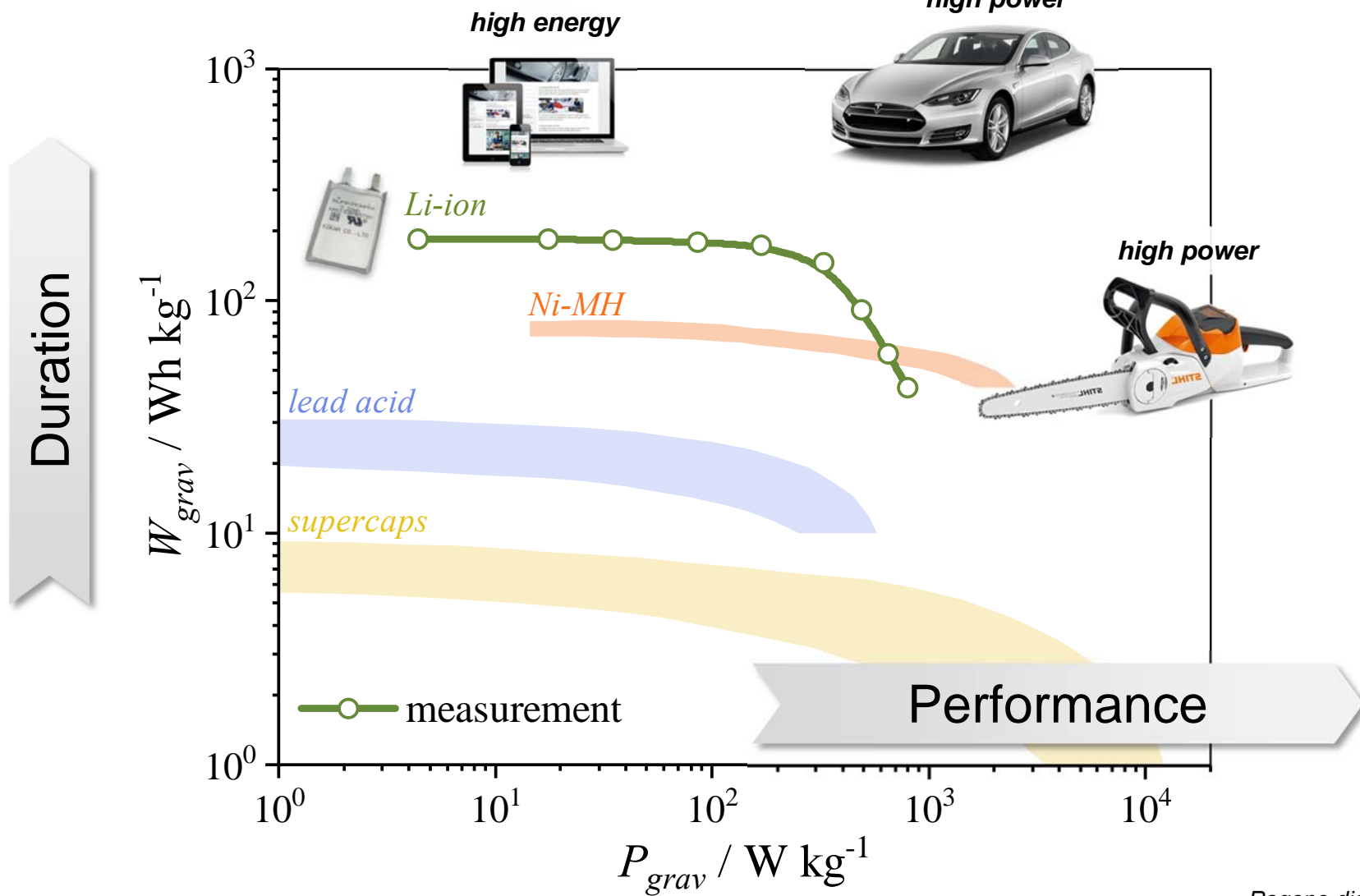
Ellen Ivers-Tiffée, Philipp Braun, Michael Weiss

Karlsruhe Institute of Technology (KIT), Germany



Motivation

Ragone Diagram

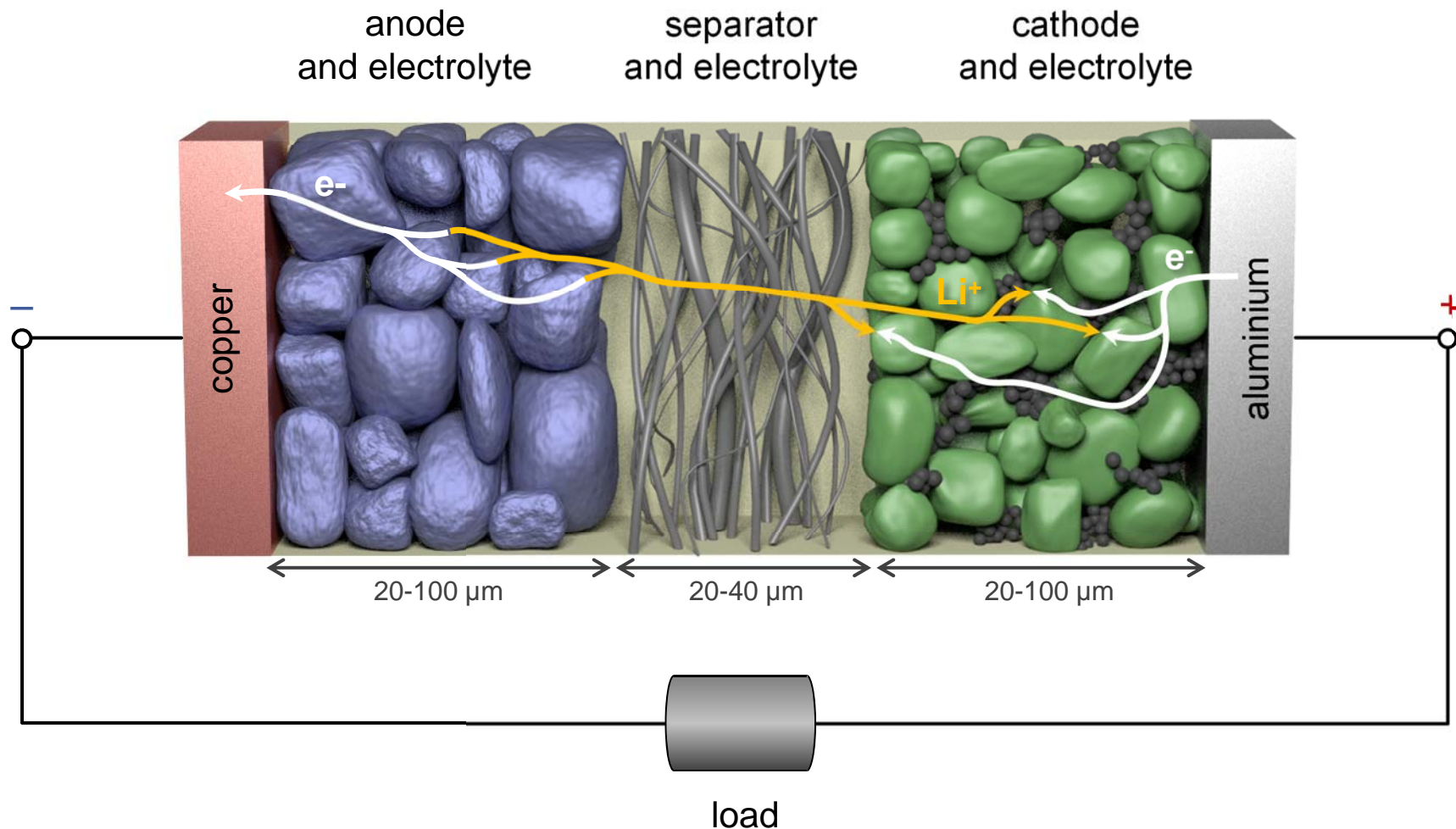


Ragone diagram on cell level



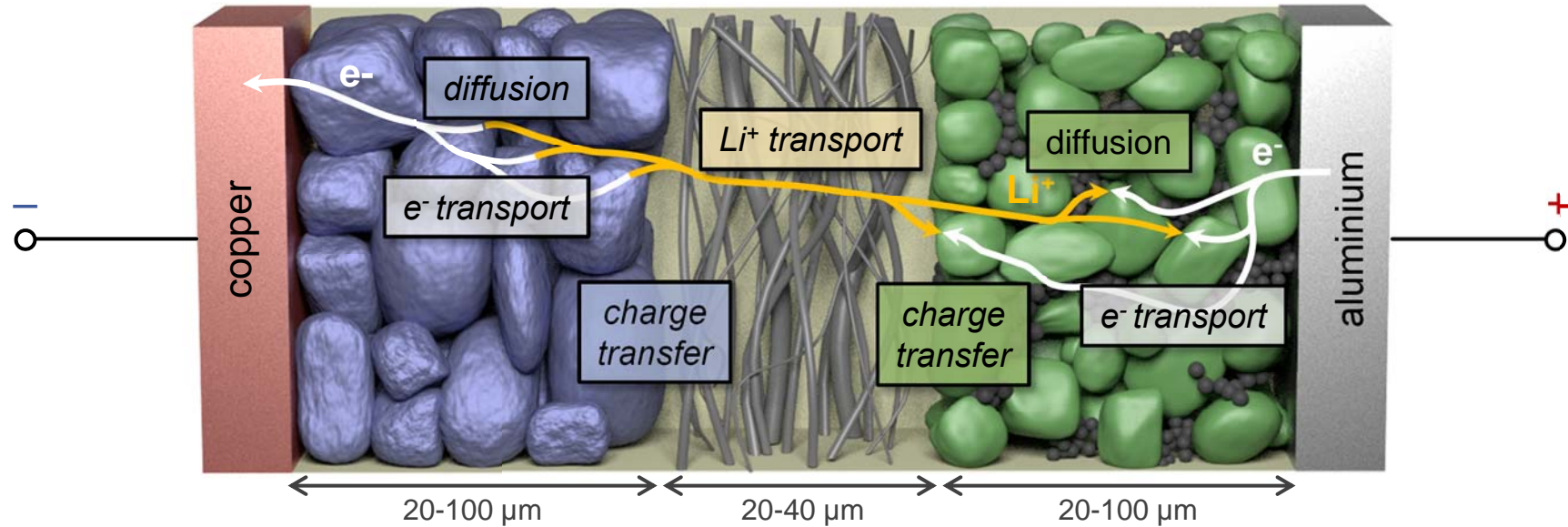
The Lithium-Ion Cell

Resistance Contributions



The Lithium-Ion Cell

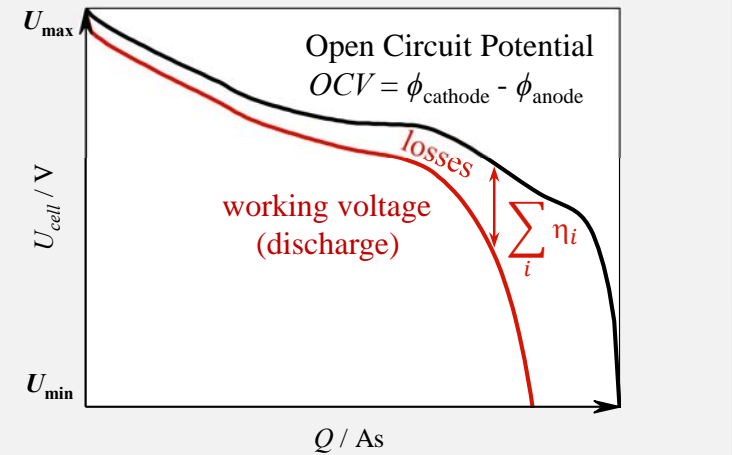
overpotential



Loss processes

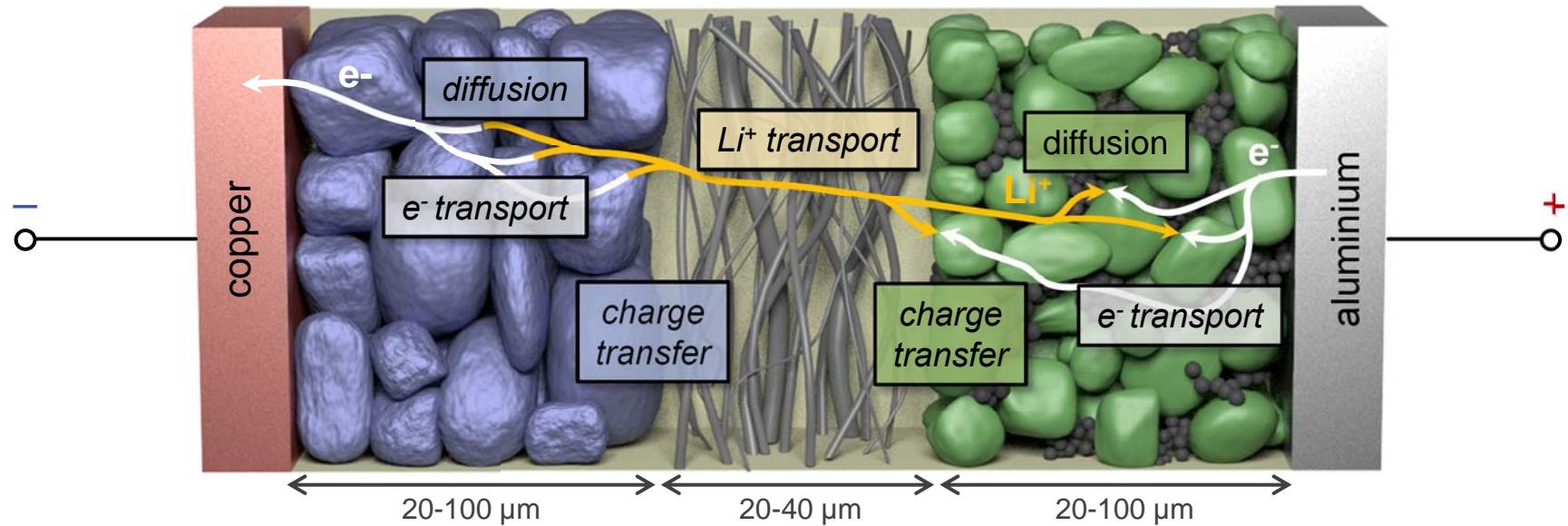
- Transport (Li^+ , e^-)
- Charge transfer (Li^+)
- Diffusion (Li^0)

$$\xrightarrow{\hspace{1cm}} \underbrace{\overline{\eta}}_{\left\{ I_{discharge} \cdot \sum_i R_i \right\}}$$



The Lithium-Ion Cell

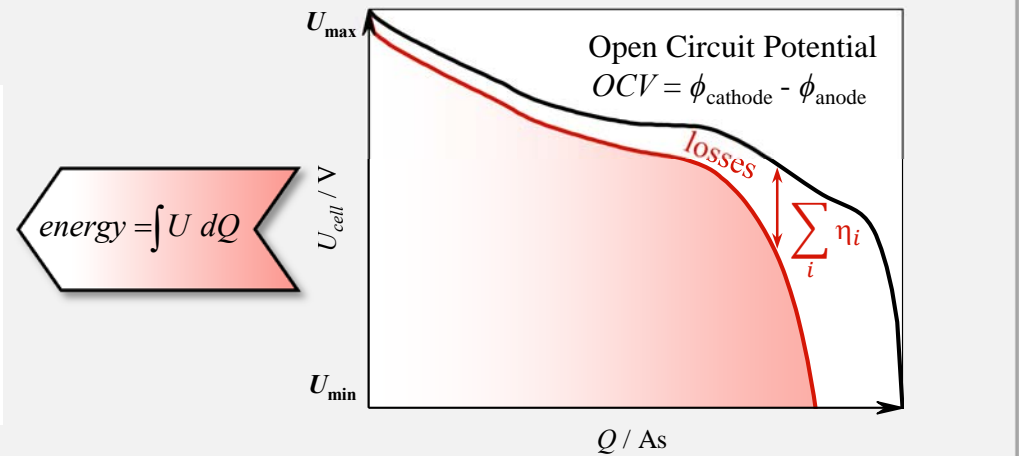
energy- and power density



Energy- and Power-density

$$W_{grav} = \frac{energy}{m_{cell}} = \frac{\int OCV - \sum_i R_i \cdot I_{discharge} dQ}{m_{cell}}$$

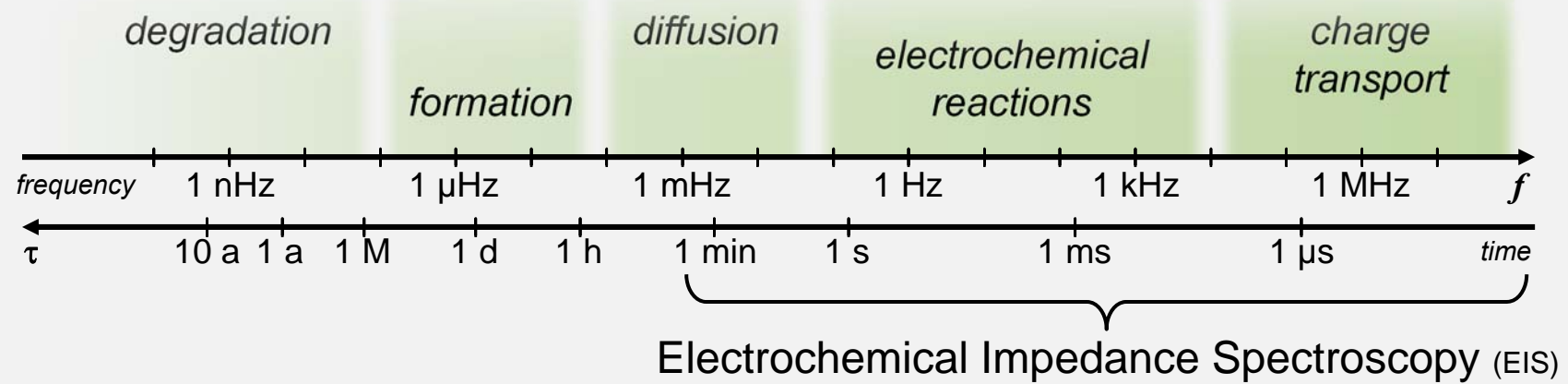
$$P_{grav} = \frac{energy}{t_{discharge} \cdot m_{cell}} = \frac{\int OCV - \sum_i R_i \cdot I_{discharge} dQ}{t_{discharge} \cdot m_{cell}}$$



Characterization of Lithium-Ion Cells

Electrochemical Impedance Spectroscopy (EIS)

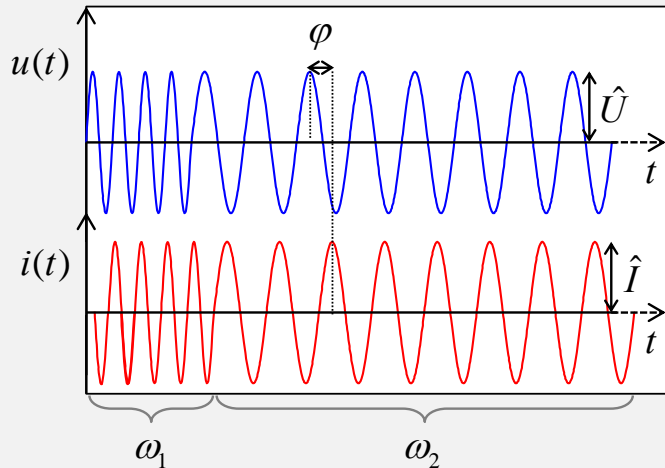
Characteristic time constants of different loss mechanisms in Lithium-ion cells:



Characterization of Lithium-Ion Cells

Electrochemical Impedance Spectroscopy (EIS)

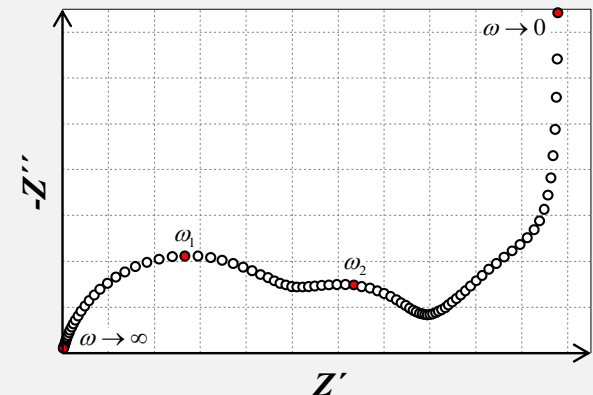
AC Small Signal Perturbation:



Frequency Response Analyzer:

$$\begin{aligned} Z(\omega) &= \frac{\hat{U}(\omega)}{\hat{I}(\omega)} \cdot e^{j\varphi(\omega)} \\ &= Z'(\omega) + jZ''(\omega) \end{aligned}$$

Nyquist Plot:

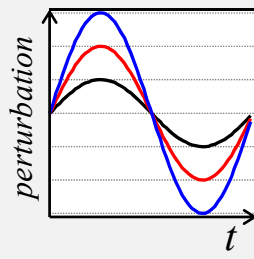


synthetic battery-like spectrum

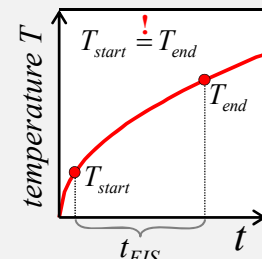
System Requirements:



causality



linearity



time invariance

Kramers-Kronig Validity Test:

$$Z_{\text{Re}}(\omega) = \frac{2}{\pi} \cdot \int_0^{\infty} \frac{\omega' \cdot Z_{\text{Im}}(\omega')}{\omega^2 - \omega'^2} d\omega'$$

$$Z_{\text{Im}}(\omega) = -\frac{2}{\pi} \cdot \int_0^{\infty} \frac{\omega \cdot Z_{\text{Im}}(\omega')}{\omega^2 - \omega'^2} d\omega'$$

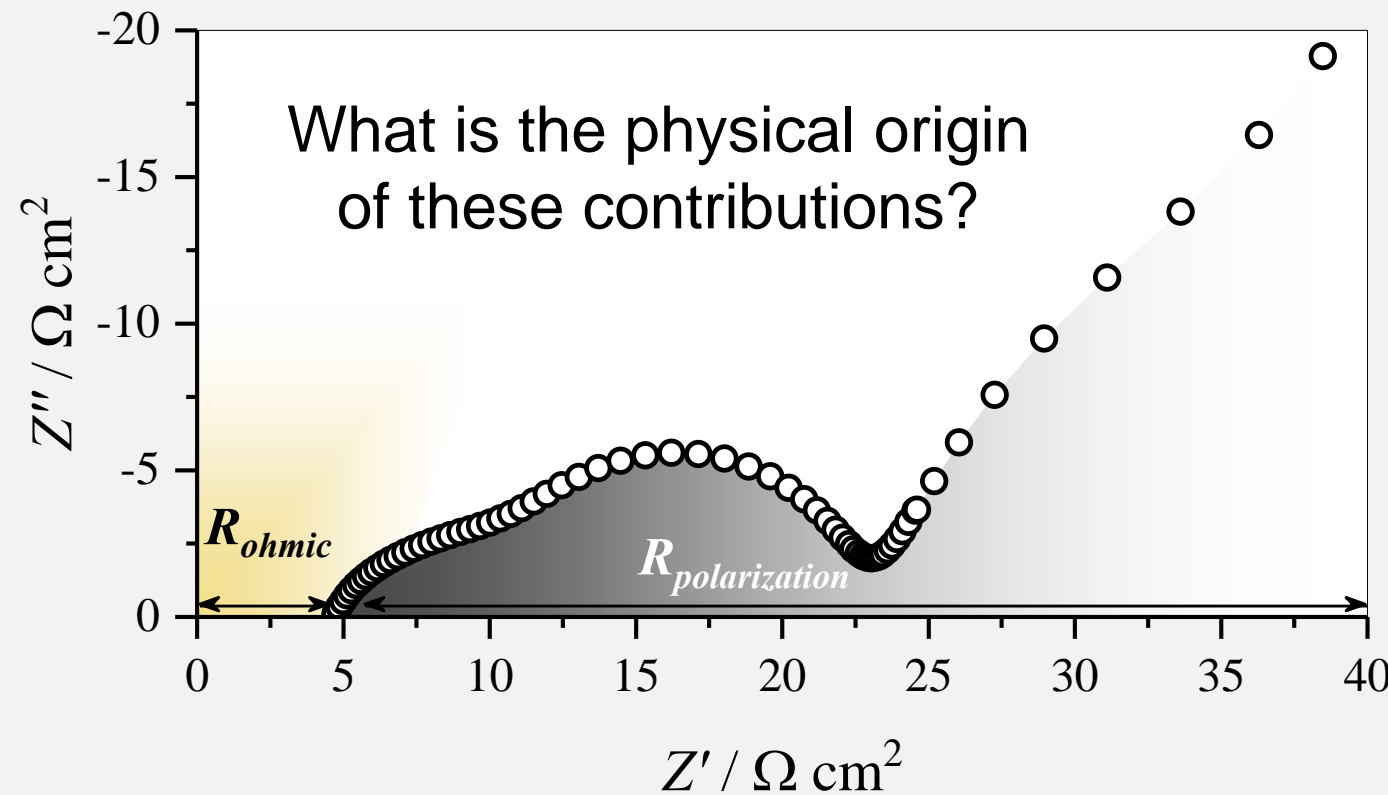
M. Schönleber, D. Klotz, and E. Ivers-Tiffée, "A Method for Improving the Robustness of linear Kramers-Kronig Validity Tests," *Electrochim. Acta*, vol. 131, pp. 20–27, 2014.



Characterization of Lithium-Ion Cells

Electrochemical Impedance Spectroscopy (EIS)

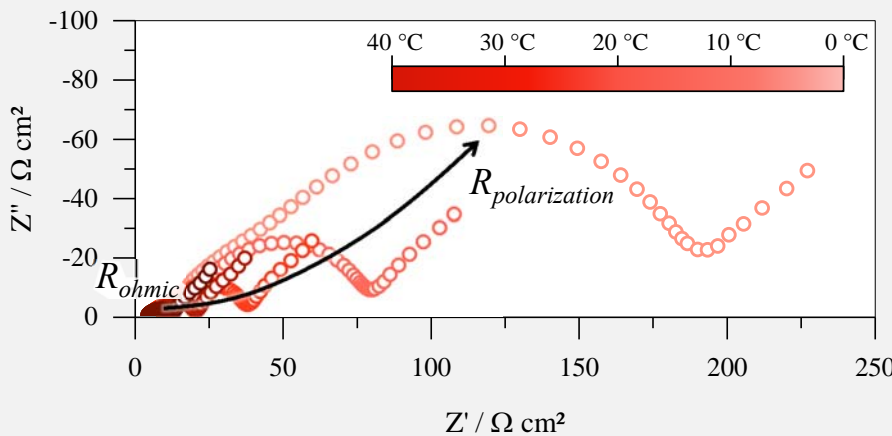
Impedance Analysis:



Characterization of Lithium-Ion Cells

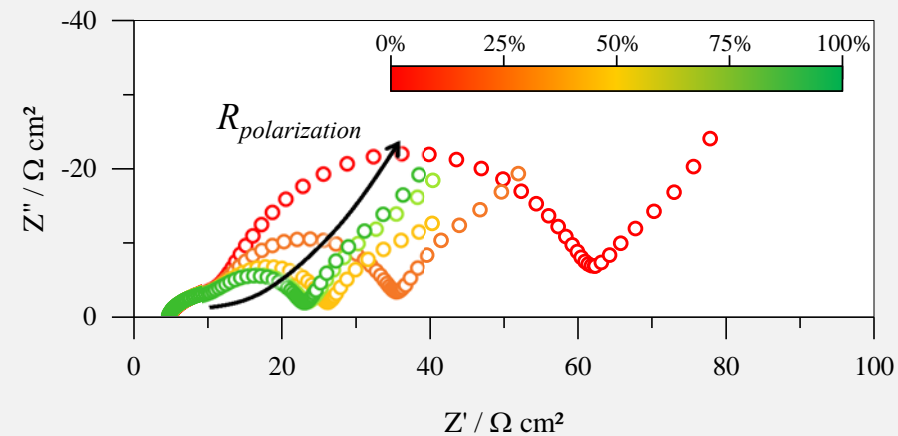
Electrochemical Impedance Spectroscopy (EIS)

Temperature variation at SoC 80 %:



→ Strong dependency of R_{ohmic} and $R_{\text{polarization}}$ on temperature

State-of-charge (SoC) variation at 25 °C:



→ Strong dependency of $R_{\text{polarization}}$ on SoC

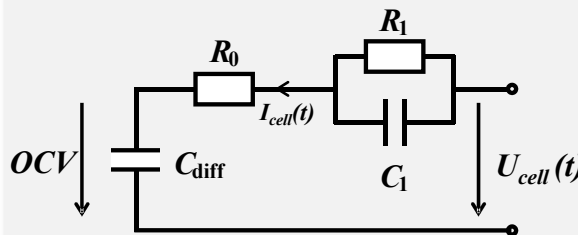
→ How to predict the performance of lithium-ion cells?

Modelling of Lithium-Ion Cells

Behavior Model

“Simple” Equivalent Circuit Model:

- *no physical meaning*
- + *simple parameterization*
- + *very short computation time*



“Advanced” Equivalent Circuit Model



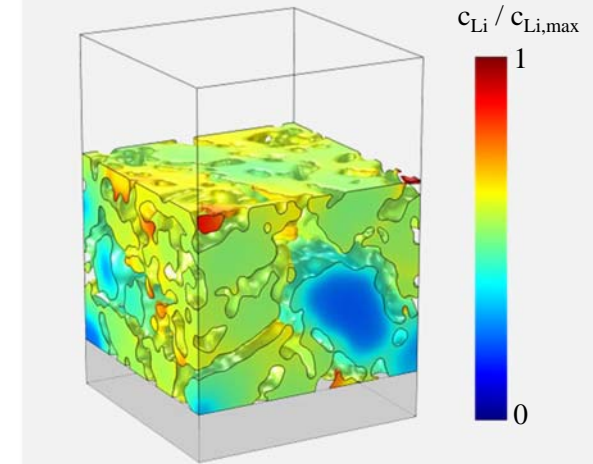
Transmission Line Models:

- + *physically motivated*
- + *feasible parameterization*
- + *short computation time*

Multiphysics Model

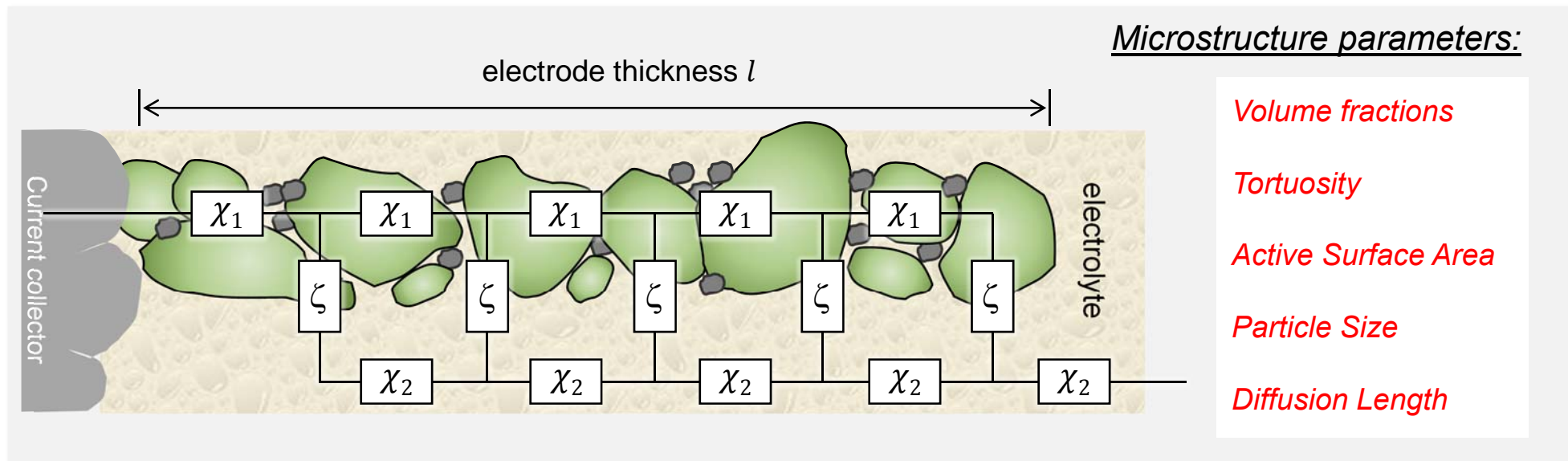
Finite Element Method:

- + *physically correct*
- *challenging parameterization*
- *long computation time*



Modeling of Lithium-Ion Cells

Transmission Line Model (TLM)



ionic path

$$\chi_2 = \frac{1}{\sigma_{ion}} \cdot \frac{\tau}{\varepsilon} \cdot \frac{1}{A}$$

τ tortuosity (pore)
 ε volume fraction of pores
 A electrode area

charge transfer

$$Z_{CT} = \frac{\rho_{CT}}{V \cdot a_{AM}} \cdot l$$

ρ_{CT} specific charge transfer resistance
 a_{AM} active surface area per unit volume
 V electrode volume

solid-state diffusion

$$\lambda = \frac{j \cdot \omega \cdot l_{Diff}^2}{D_{Diff}}$$

l_{Diff} diffusion length
 D_{Diff} diffusion coefficient
 C_0 differential capacity

$$Z_{Diff} = \frac{1}{C_0} \cdot \frac{l_{Diff}}{D_{diff}} \cdot \frac{I_0 \cdot \sqrt{\lambda}}{\sqrt{\lambda} \cdot I_1 \cdot \sqrt{\lambda}}$$

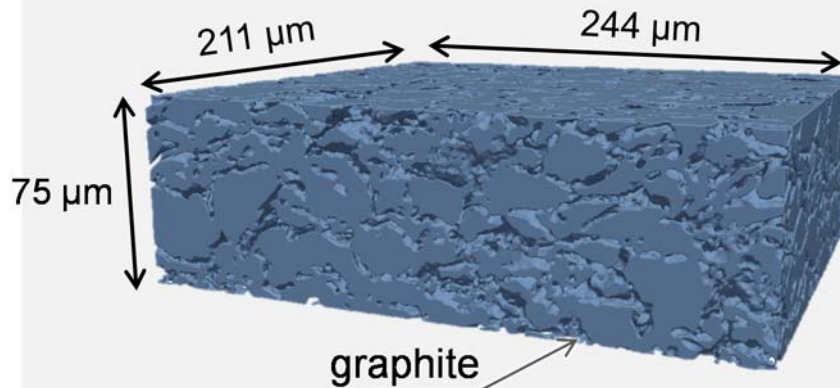
Finite-Space Warburg Impedance



Characterization of Lithium-Ion Cells

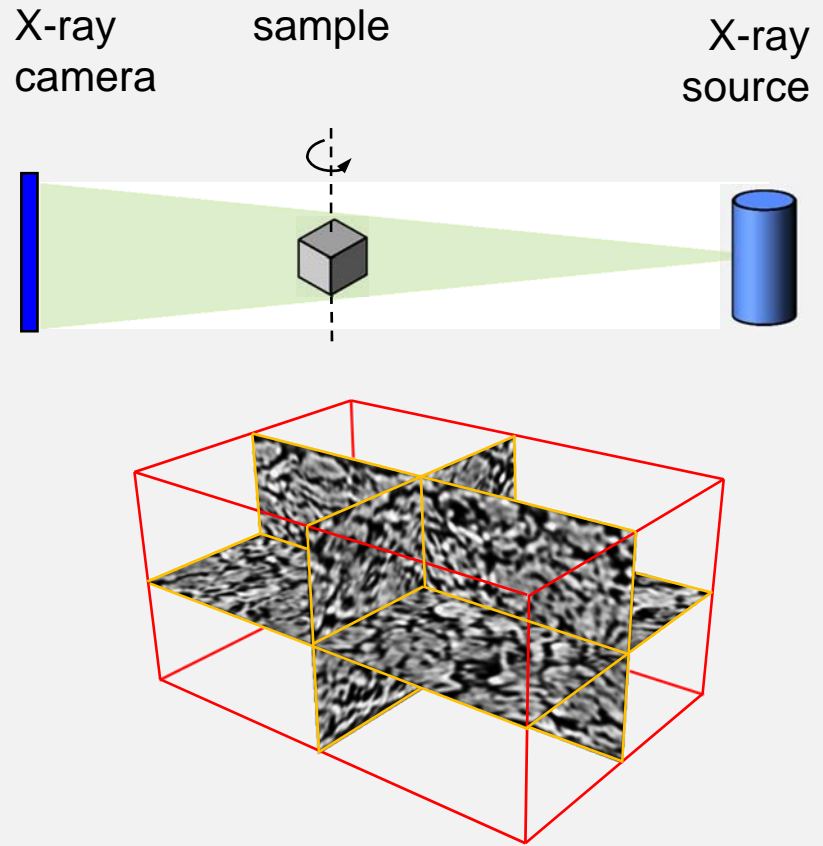
Microstructure: Anode

Anode: Graphite



electrode thickness	$l_{\text{electrode}}$	= 90 μm
volume fraction	$\varepsilon_{\text{graphite}}$	= 0.75
	$\varepsilon_{\text{pore}}$	= 0.25
tortuosity	τ_{pore}	= 5.12
active surface area	a_{graphite}	= 0.314 μm^{-1}
particle size	$d_{\text{graphite,vol-av}}$	= 12.07 μm

X-ray nano-tomography:

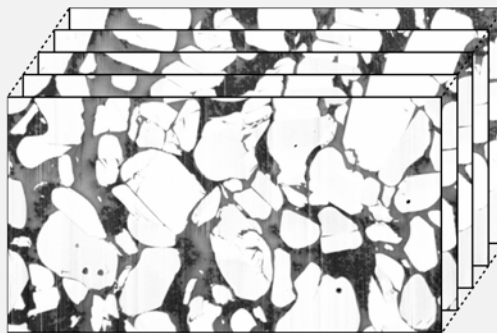
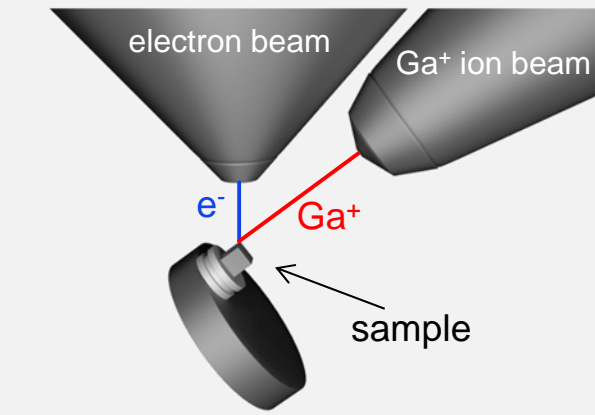


M. Ender, J. Joos, A. Weber, and E. Ivers-Tiffée, "Anode microstructures from high-energy and high-power lithium-ion cylindrical cells obtained by X-ray nano-tomography," *J. Power Sources*, vol. 269, pp. 912–919, 2014.

Characterization of Lithium-Ion Cells

Microstructure: Cathode

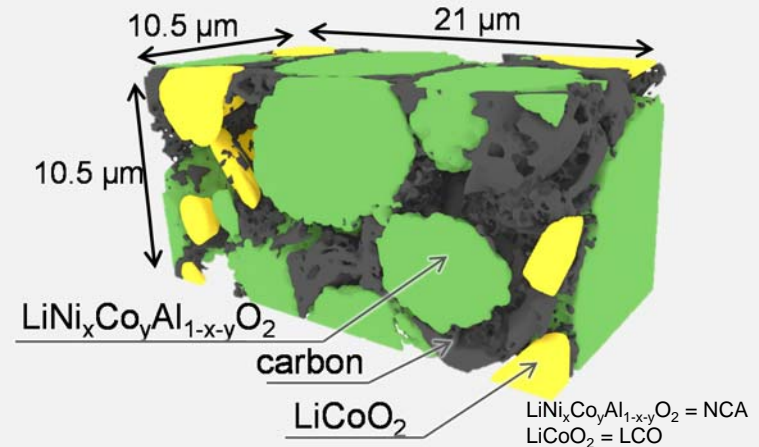
Focused ion beam (FIB) tomography:



M. Ender, J. Joos, T. Carraro, and E. Ivers-Tiffée, "Three-dimensional reconstruction of a composite cathode for lithium-ion cells," *Electrochim. commun.*, vol. 13, no. 2, pp. 166–168, 2011.

M. Ender, J. Joos, T. Carraro, and E. Ivers-Tiffée, "Quantitative Characterization of LiFePO₄ Cathodes Reconstructed by FIB/SEM Tomography," *J. Electrochim. Soc.*, vol. 159, no. 7, pp. A972–A980, Jan. 2012.

Cathode: NCA/LCO Blend

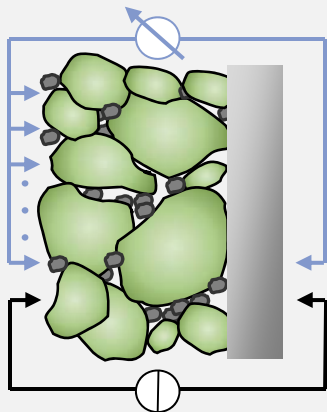


electrode thickness	$l_{\text{electrode}}$	= 75 μm
volume fraction	ε_{AM}	= 0.57
	$\varepsilon_{\text{carbon}}$	= 0.17
	$\varepsilon_{\text{pore}}$	= 0.26
tortuosity	τ_{pore}	= 4.29
active surface area	a_{AM}	= 0.73 μm ⁻¹
particle size	$d_{\text{AM,vol-av}}$	= 4.06 μm

Characterization of Lithium-Ion Cells

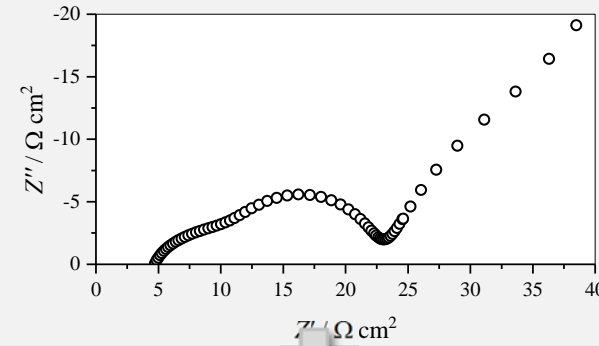
Parametrization of transition line models

e⁻ conductivity

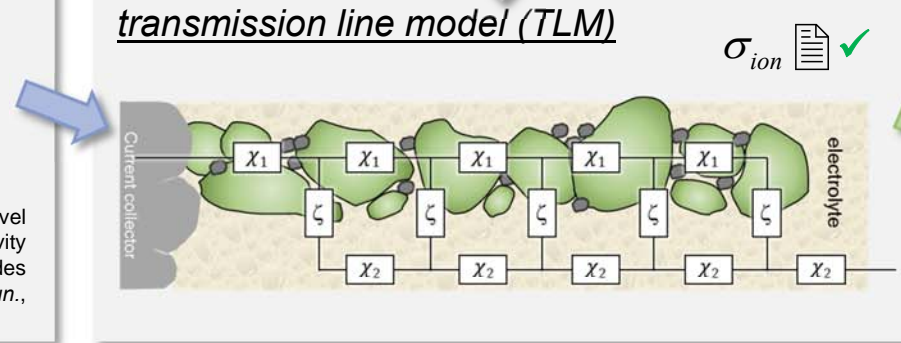


electronic conductivity σ_{e^-}

impedance measurement



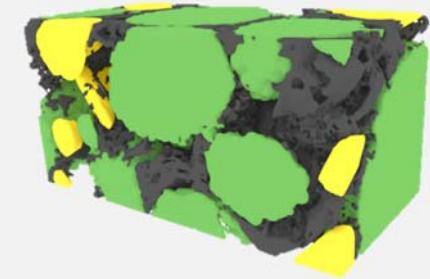
transmission line model (TLM)



σ_{ion}

M. Ender, A. Weber, and E. Ivers-Tiffée, "A novel method for measuring the effective conductivity and the contact resistance of porous electrodes for lithium-ion batteries," *Electrochim. commun.*, vol. 34, pp. 130–133, 2013.

microstructure



ε volume fractions

a_V active surface area

τ tortuosity

pS particle size

l electrode thickness

M. Ender, J. Joos, T. Carraro, and E. Ivers-Tiffée, "Quantitative Characterization of LiFePO₄ Cathodes Reconstructed by FIB/SEM Tomography," *J. Electrochem. Soc.*, vol. 159, no. 7, pp. A972–A980, Jan. 2012.

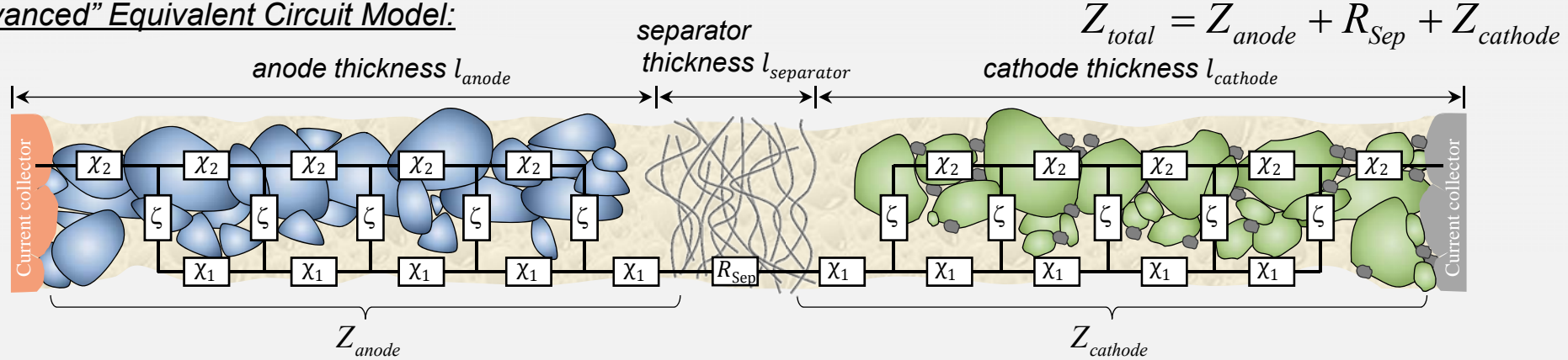
conclusion

Electrochemical and microstructure parameters for anode and cathode are determined

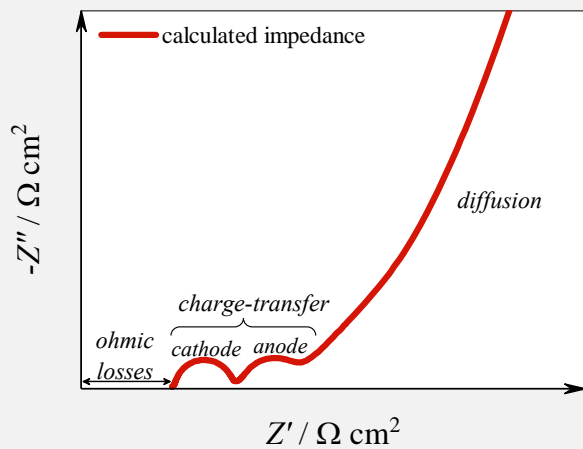
Li-Ion Battery Model

Homogenized 1D Model

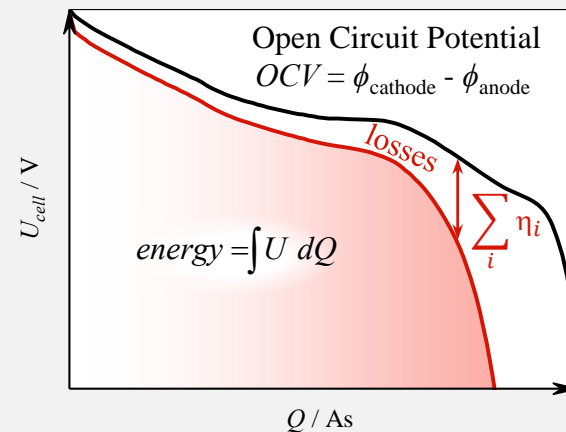
"Advanced" Equivalent Circuit Model:



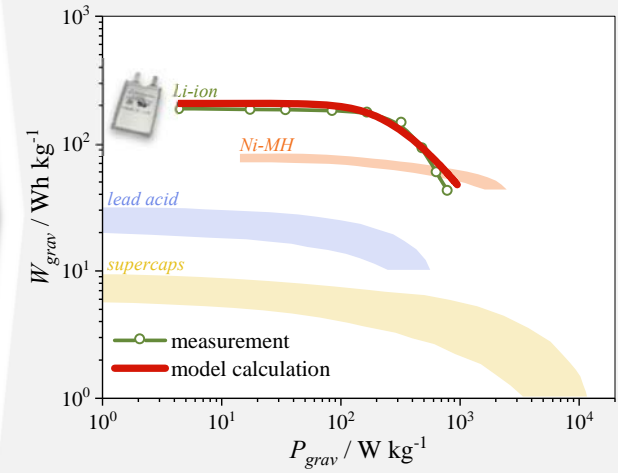
Impedance:



Discharge curve:



Ragone Plot:

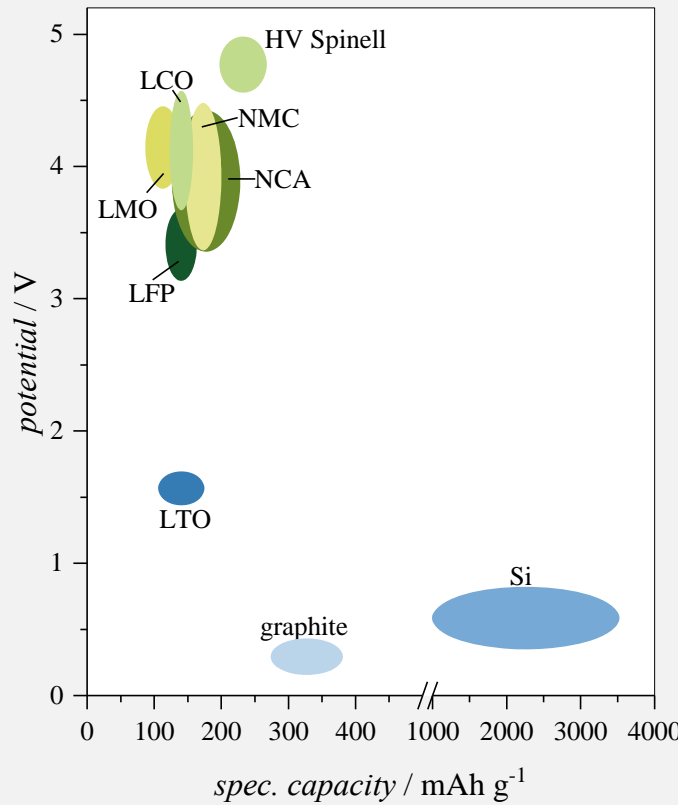


Model-Based Optimization

Energy Optimization

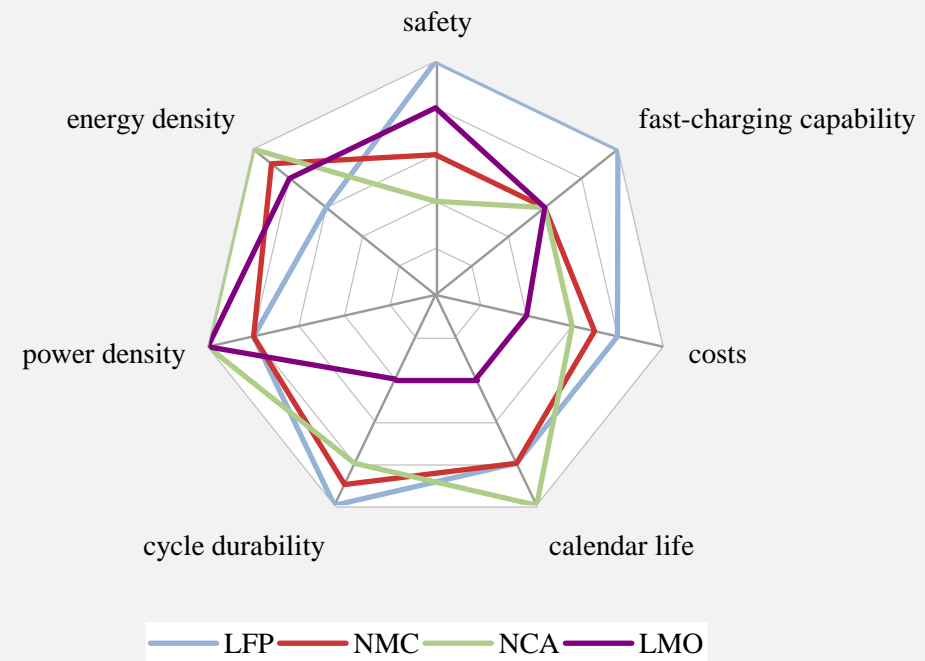
$$energy = \int \phi_{cathode} - \phi_{anode} dQ$$

y-axis x-axis



Relevant Design Factors

Example: cathode active materials



LFP: LiFePO_4

NMC: $\text{LiNi}_{1-x-y}\text{Co}_x\text{Mn}_y\text{O}_2$

HV Spinell: $0.3\text{Li}_2\text{MnO}_3 \quad 0.7\text{LiNi}_{0.5}\text{Mn}_{1.5}\text{O}_4$

NCA: $\text{LiNi}_{1-x-y}\text{Co}_x\text{Al}_y\text{O}_2$

LMO: LiMn_2O_4

Model-Based Optimization

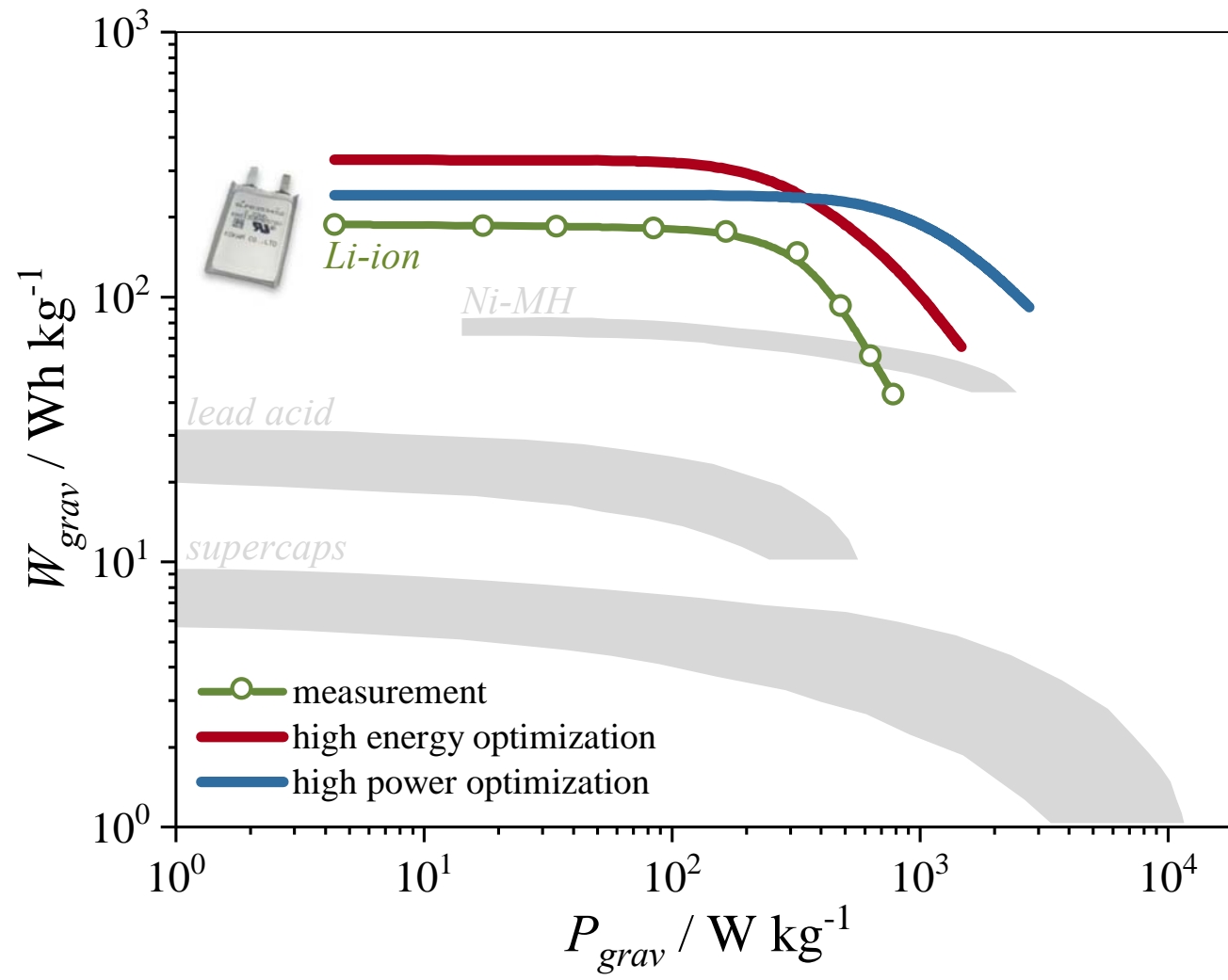
→ change parameters of “state-of-the-art” active materials

	Anode	Cathode	Passive Components
<p><u>High Energy</u> Optimization</p> <p>Increase capacity Reduce mass</p>	<p><i>Specific Capacity:</i></p> <p>graphite (350 mAh g^{-1}) + 30% graphite + 15% Si (450 mAh g^{-1})</p>	<p><i>Specific Capacity:</i></p> <p>LCO / NCA (145 mAh g^{-1}) + 40% NMC811 (200 mAh g^{-1})</p> <p><i>Volume Fractions:</i></p> <p>57% NCA/LCO + 20% 70% NMC811</p>	<p><i>current collectors:</i></p> <p>$I_{cc} = 20 \mu\text{m}$ - 50% $I_{cc} = 10 \mu\text{m}$</p>
<p><u>High Power</u> Optimization</p> <p>Increase surface area Reduce electrode thickness</p>	<p><i>Particle Size:</i></p> <p>$12.1 \mu\text{m}$ - 95% $0.5 \mu\text{m}$</p> <p><i>Thickness:</i></p> <p>$90 \mu\text{m}$ - 55% $40 \mu\text{m}$</p>	<p><i>Particle Size:</i></p> <p>$4.1 \mu\text{m}$ - 88% $0.5 \mu\text{m}$</p> <p><i>Thickness:</i></p> <p>$75 \mu\text{m}$ - 60% $30 \mu\text{m}$</p>	<p>+</p> <p>all high energy optimization steps</p>



Model-Based Optimization

→ change parameters of “state-of-the-art” active materials

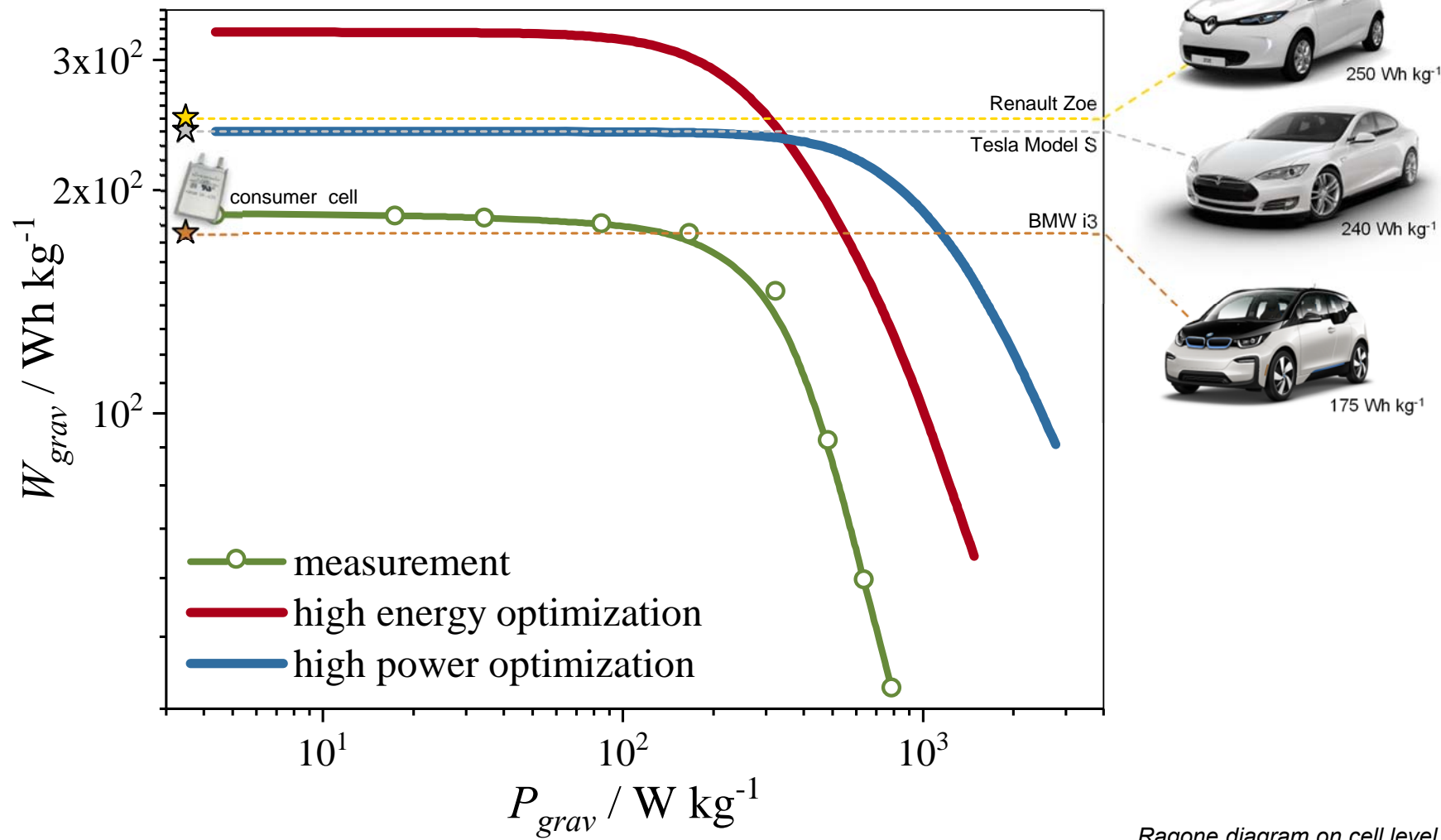


Ragone diagram on cell level



Model-Based Optimization

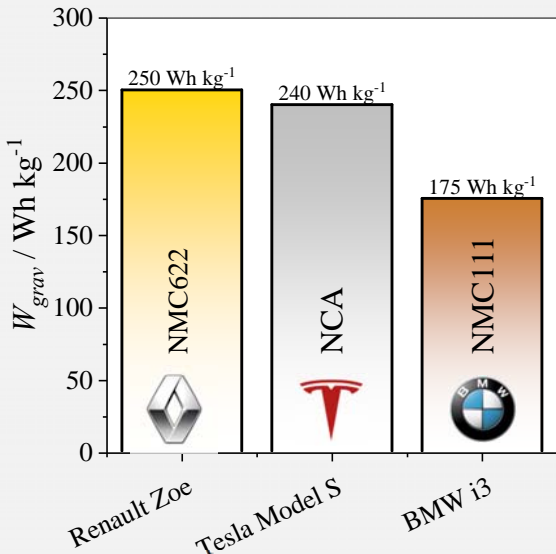
→ change parameters of “state-of-the-art” active materials



State-of-the-art electric vehicles

comparison from cell to car

Energy-Density: Cell-Level

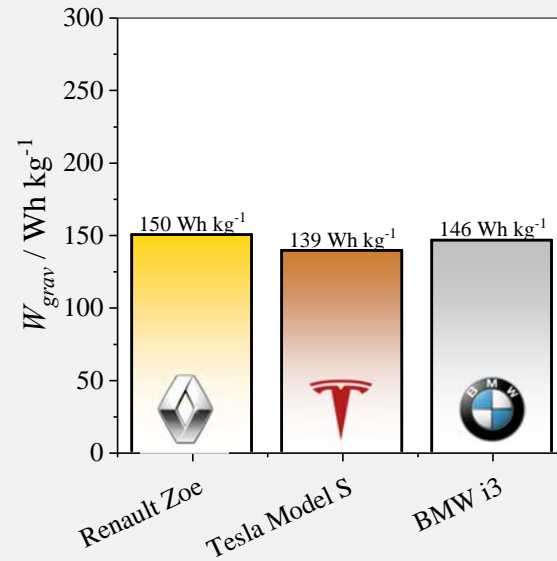


192
pouch
cells

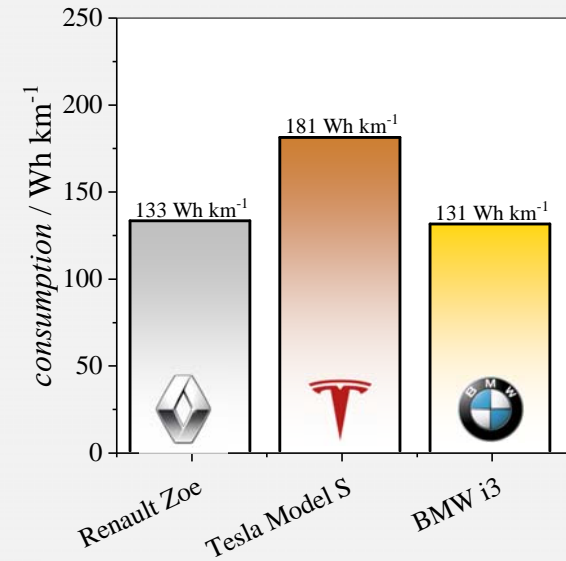
7104
cylindrical
cells

96
prismatic
cells

Energy-Density: Battery-Level

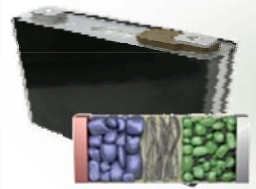


Consumption

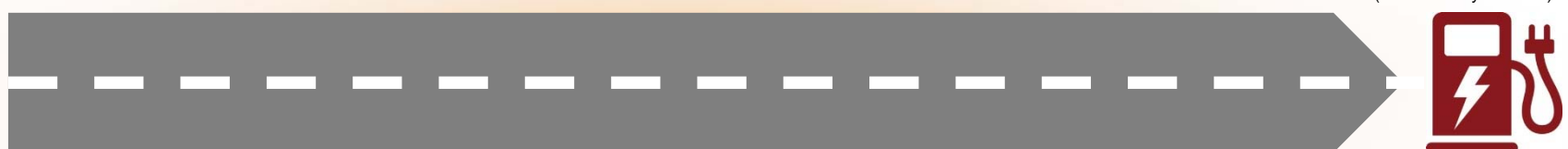
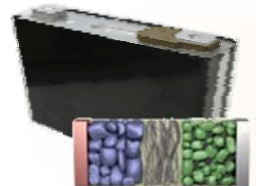


Electric Range Prediction

State-of-the-art Battery



Future Prospects





Thank you very much for your kind attention!

Acknowledgements:
Research Partners and Team IAM-WET



Bundesministerium
für Bildung
und Forschung



Deutsche
Forschungsgemeinschaft



Institute for Applied Materials
Materials for Electrical and Electronic Engineering

www.iam.kit.edu/wet